# ADDITIVE MANUFACTURING AND VULCANIZATION OF CARBON BLACK–FILLED NATURAL RUBBER–BASED COMPONENTS

SEBASTIAN LEINEWEBER,[1,*] LION SUNDERMANN,[2,*] LARS BINDSZUS,[1] LUDGER OVERMEYER,[1]
BENJAMIN KLIE,[2] HEIKE WITTEK,[2] ULRICH GIESE[2]

[1]INSTITUT FÜR TRANSPORT-UND AUTOMATISIERUNGSTECHNIK
[2]DEUTSCHES INSTITUT FÜR KAUTSCHUKTECHNOLOGIE E.V.

RUBBER CHEMISTRY AND TECHNOLOGY, Vol. 95, No. 1, pp. 46–57 (2022)



## ABSTRACT

Additive manufacturing of thermoplastics or metals is a well-approved sustainable process for obtaining rapidly precise and individual technical components. Except for crosslinked silicone rubber or thermoplastic elastomers, there is no method of additive manufacturing of elastomers. Based on the development of the additive manufacturing of elastomers (AME) process, the material group of rubber-based cured elastomers may gain first access to the process field of three-dimensional (3D) printing. Printing and crosslinking of rubber is separated into two steps. In the first step, printing is realized by extrusion of the rubber by using a twin-screw extruder, which works according to the derived fused-filament-fabrication principle. In the second step, the component is vulcanized in a high-pressure hot-air autoclave. Because of the plastic flow behavior of non–crosslinked rubber materials, a thermoplastic shell is probably needed to maintain the geometry and position of the additively manufactured rubber. In this way, one layer of thermoplastic and one layer of rubber are printed alternatingly until the component is finished. Afterward, the manufactured binary component is placed in an autoclave to obtain the elastomer after vulcanization under a hot-air and high-pressure atmosphere. Then, the thermoplastic shell is removed from the elastomer and can subsequently be recycled. As compared with conventional thermoplastics, the high viscosity of rubber during processing and its instable shape after extrusion are challenging factors in the development of the AME. This contribution will show a modified 3D printer; explain the printing process from the designed component, via shell generation, to the vulcanized component; and show first printed components. [doi:10.5254/rct.21.79906]

## INTRODUCTION

Additive manufacturing of thermoplastics or metals has become state of the art and is used in a wide range of areas, including automotive engineering, aerospace, and the manufacturing of medical products.[1] In contrast, the development of processes for the additive manufacturing of elastomers is still in its beginnings. Until now, processes of additive manufacturing of elastomers have been based on the processing of either thermoplastic elastomers[2] or cross-linked silicone rubbers,[3] such as nanosilica composite elastomers[4] or poly(2-methoxyethylacrylate)-silica composite elastomers.[5,6] However, to date, the additive manufacturing of rubber-based elastomers in particular has posed major challenges to science. In one project, ground tire rubber was printed as a filler in a polymer matrix.[7] Otherwise, in parallel with the work carried out here (as far as the authors are aware), only Drossel et al. are working in the field of extrusion-based additive manufacturing of unvulcanized rubber-based elastomers.[8] The processing method used in their research differs fundamentally from the additive manufacturing of elastomers (AME) process and is currently limited to acrylonitrile–butadiene rubber–based rubber compounds with a certain viscosity range.[9]

In general, rubber-based carbon black–filled elastomer materials offer a wide range of possible applications in the industry. Rubber is used in particular for seals,[10] dampers,[11] and tires.[12] In comparison with natural or other synthetic rubbers, silicone rubber shows an especially highly temperature-dependent chemical resistance and mechanical behavior, which has a negative impact on the use of these materials as an alternative to conventional rubber.[13] Additive manufacturing is used for the production of prototypes[14] as well as for manufacturing spare parts.[15] In particular, the

*Corresponding authors. Emails: sebastian.leineweber@ita.uni-hannover.de, Lion.Sundermann@DIKautschuk.de

production of spare parts can be a sustainable aspect[16,17] for the rubber industry. Rubber ages during storage,[18] so that stored rubber components are no longer usable after a few years because of their embrittlement. With just-in-time production, this waste of resources can be avoided.[19] The aging behavior of rubber appears to be particularly disadvantageous if the production of plant and plant-specific spare parts is discontinued and stocks of rubber-based spare parts are no longer usable after a few years. As a consequence, otherwise functioning plants have to be shut down. This behavior can be countered by the sustainable use of additive manufactured spare parts, which have proven to be economically and particularly ecologically profitable for companies and society as a whole.[16,17]

These facts make it clear that there must be a scientific interest in creating a process for additive manufacturing of rubber-based carbon black–filled elastomers. In contrast to conventional thermoplastics, the high viscosity of rubber[13] and the plastic flow behavior[20] of nonvulcanized rubber pose major challenges for additive manufacturing of carbon black–filled rubber elastomers. Processing of a highly loaded polymer is necessary to reduce the extrudate distortion and die swell after passing the nozzle of the extruder. However, a high carbon black[13] loading but also a small particle size and high structure of the used carbon black increase the viscosity,[21] which requires sufficient torque of the extruder, so that the use of conventional thermoplastic extruder from the three-dimensional (3D)–printing field is not suitable.

This work is based on the principle of AME, a process developed by Wittek et al.[22] In this process, a thermoplastic, which acts as a shell material, and rubber are printed in layers in serial printing. Thus, in each layer, the printed rubber is protected from flowing by a thermoplastic shell.[22] The process is based on fused filament fabrication, a method used for additive manufacturing of thermoplastics.[23,24] The 3D printer used is a fused deposition modeling printer that has been extended by a small twin-screw extruder to deposit unvulcanized rubber in strands and layers on a printing table. Once the components have been printed, they must be vulcanized in their shells in a high-pressure hot-air autoclave.[22] After vulcanization, the elastomer component is dimensionally stable,[13] and the shell can be removed. The setup of the 3D printer was shown in detail in a previous publication. Initial extrusion tests have also been carried out to determine the material throughput of the extruder.[25]

At the beginning of this article, the output equipment and the materials used for printing are described. Subsequently, the printer developed for the AME process is presented. Following, the process of the generation of a computer-aided design (CAD) file to the finished vulcanized component is briefly described using a process chain. However, the core of this work is an algorithm for generating a printable G-Code for the AME process and a materials science evaluation of the process. The first print results are subsequently displayed.

Preliminary tests have shown that a shell is not necessary for every component. The tensile specimens highlighted in this article are stamped out from additive manufactured rubber plates, which were therefore printed without shell, and are then compared with specimens that were stamped out from a conventionally produced pressed rubber plate. In particular, the adhesive behavior of the printed rubber strands among each other is evaluated without having to take complex geometries into account. Afterward, the influence of the shell is shown by printed cuboids. Finally, a conclusion of the results is given.

## EXPERIMENTAL

### EXTRUDER SPECIFICATIONS

The rubber extruder is a co-rotating 9-mm twin screw extruder with a conveying screw design without any kneading elements from Three-Tec GmbH (Seon, Switzerland) that provides a maximum torque of 13 Nm. The pitch of the screws is 9, and the relation L/D is 20. Different

rotational speeds can be adjusted from 0–200 rpm. The temperature can be controlled in three zones separately up to 200 °C.

### ADDITIVE MANUFACTURING UNIT FOR THERMOPLASTICS

The basic 3D printer is a former CNC milling machine converted to a fused filament fabrication printer (model M3-3D, BZT Maschinenbau GmbH, Leopoldshöhe, Germany). It has two high-temperature print heads for thermoplastic material that can be heated up to 400 °C. The size of the printing area is 500 mm × 500 mm × 250 mm, and the printing plate of this 3D printer model is stationary. Thus, a layer change is achieved by moving the print heads up by one unit of length. The repeatability in the printing process is 0.03 mm. The printing bed is a carbon printing plate that can be heated up to 120 °C in a closed construction space. Consequently, the construction space can be heated by the plate.

### HIGH-PRESSURE HOT-AIR AUTOCLAVE

A high-pressure hot-air autoclave from Zirbus Technology GmbH (Bad Grund, Germany) with the designation HDA-H 65-10-180 is used for vulcanization of the rubber components. The autoclave has a pressure chamber volume of 62 L. Vulcanization itself can be performed at a pressure of up to 9.5 bar and up to 185 °C, making this autoclave ideal for the vulcanization of rubber.

### MATERIALS

The natural rubber–based recipe used in this study is used for windshield wiper blades. The formula is based on the SVR CV 50 natural rubber with a Mooney viscosity ML (1+4) at 100 °C of 50 MU ± 5. Corax N 550 with a statistical thickness surface area (STSA) of 39 $m^2/g$ and an oil absorption number (OAN) of 121 mL/100 g is used as semieffective filler. The carbon black content is 40 phr. Additional additives and a sulfur accelerator–based curing system complete the formula. Mooney viscosity of the rubber compound is determined to Mooney ML (1+4) at 100 °C by means of a Monsanto MV 2000 E viscometer to 97 MU. It was measured with the large rotor, at a preheating time of 1 min and a testing time of 4 min. The shells are printed with a water-soluble polyvinyl alcohol (PVA) filament, which is printed at a nozzle temperature of 220 °C.

## RESULTS AND DISCUSSION

### SETUP FOR THE AME PROCESS

Since the rubber viscosity is too high, even when heated, direct printing via integrated print heads of the 3D printer is not possible. Therefore, the 3D printer has to be modified for the AME process. For this purpose, a twin-screw extruder is integrated into the existing 3D printer. The extruder has a sufficiently high torque to extract and print rubber. The extruder is assembled directly on the traversing unit of the 3D printer as shown in Figure 1.

Because the extruder is approximately 12 kg heavier than the two original thermoplastic print heads of the 3D printer, it was assembled as close as possible to the balance point of the traversing unit, minimizing the tilting moment, thus preventing vibrations during the printing process that might negatively affect printing resolution. The extruder is directly connected to the movement of the 3D printer, and only the feeding of rubber has to be controlled separately. The original print heads were assembled in front of the extruder. The control unit of the 3D printer allows the selection of a print head for thermoplastic material or the extruder for rubber. However, the controller does not directly give the order for printing to the extruder. It sends the signal to the extruder's

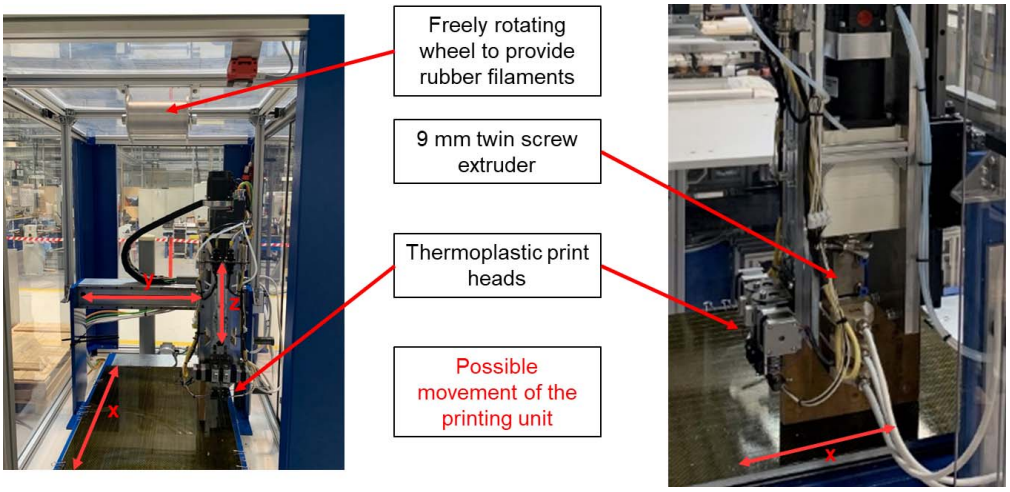


FIG. 1. — Setup of the new additive manufacturing plant for the AME process.

additionally postimplemented control unit, which activates the extruder. An additional touch panel on the control unit of the extruder enables controlling of the feed rate by adjusting the rotational speed of the screws. In general, speed values are fixed before the printing process starts, so that the control unit of the extruder only receives an order to start or to stop printing.

To ensure a continuous material feeding of the extruder, a freely rotating wheel is installed above the extrusion unit, which is able to follow the movement of the 3D-printing unit in the *x* direction. The roller is wrapped with rubber filament before printing. During the printing process, the material is fed by the extruder and continuously processed. Only a continuous material feed ensures a continuous material flow, which is required for a constant printing speed and a printed layer with a constant volume and a stable geometry.

## THE PROCESS CHAIN

To manufacture rubber components by additive manufacturing, the steps shown in Figure 2 must be carried out. First, a component must be designed using CAD software and then converted into the STL format, which has become established in additive manufacturing. Then, with the help of the software Autodesk Netfabb Premium 2019, a shell with a freely selectable thickness is generated automatically and also converted into the STL format. The shell is used to keep the nonvulcanized rubber in shape during the 3D-printing process and before vulcanization. Alternatively, the required shell can also be designed manually.

The freeware Slic3r is used to generate a G-Code. However, the software has two significant disadvantages for the AME process. On one hand, the software uses only a travel-optimized strategy, the so-called ABBA strategy, for generating a G-Code. This means that, first, a shell (A) is printed in one layer, then a core (B) in the same layer; in the next layer, first a core (B) is printed, followed by a shell (A), and so on. This printing behavior would result in possibly nongeometrically stable rubber layers, which are printed before the thermoplastic in every second printing step, making this strategy unsuitable for the AME process. On the other hand, the software does not provide a setting for different resolutions. This means different layer thicknesses for the rubber extruder and the thermoplastic print head are not possible, although the thermoplastics could be printed with a much thinner layer height than the rubber. This should be preferably done to

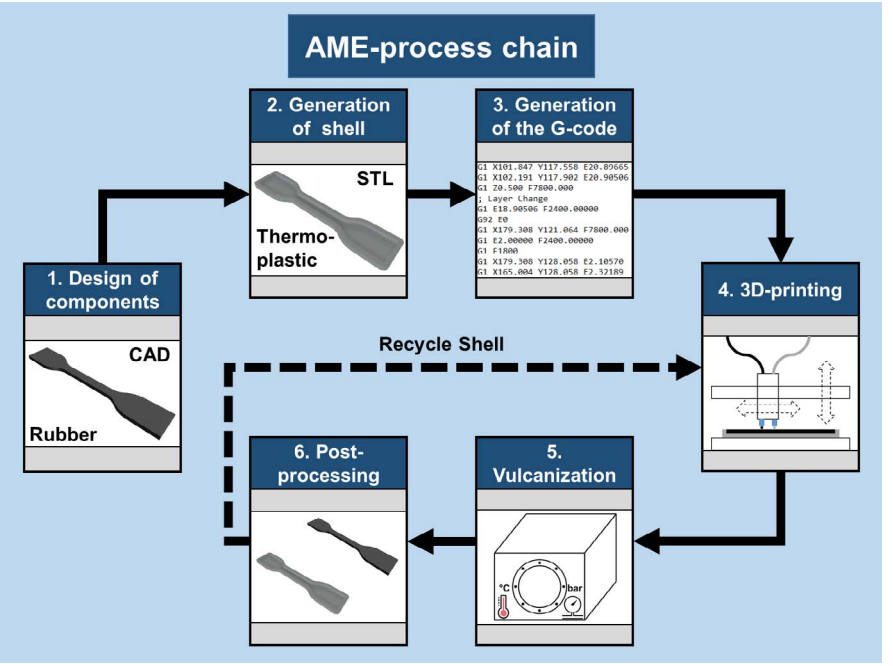


FIG. 2. — Process chain of the AME process.

minimize imprints of layer structures covered by the rubber surface that occur due to the flowability of the rubber material until vulcanization has stabilized its geometry.

Therefore, a G-Code for the shell and the component should be generated separately. It is important to ensure that the offset between the thermoplastic print head and the rubber extruder is also entered into the slicing software so that the component is located inside the shell during printing. Furthermore, the resolution of the thermoplastic shell must be a fraction of the resolution of the rubber component so that layers are always completed after the rubber has been printed. For a rubber resolution of 0.9 mm, either a resolution of 0.3 mm or 0.15 mm of a shell would be possible. An even finer resolution is also conceivable, if the 3D printer used technically permits this.

To merge the two generated G-Codes back into one G-Code, a software with a sorting algorithm was developed, which is described in the next section and enables the generation of a G-Code that corresponds to a printing strategy of the type xA→B→xA→B, whereby x represents the number of layers of the thermoplastic material to be printed. The print speed of 20 mm/s is set in Slic3r. Preliminary tests have shown that a printing speed of 20 mm/s is suitable for the manufacturing of rubber.

After the G-Code has been modified by the independently developed software for the AME process, 3D printing can begin. The selected rubber is printed at a temperature of 100 °C, and the material of the shell is printed at a temperature of 220 °C. The 3D printing is followed by vulcanization in a high-pressure hot-air autoclave. The selected parameters are described in more detail in the section on the analysis of the components. After vulcanization, components are released from their shells and, if necessary, cleaned of thermoplastic residues in postprocessing.

## MODIFICATION OF THE G-CODE

First, the information on the layer thickness of a component and its shell and on the thickness of the bottom of the shell have to be entered in a graphical user interface. Then, the G-Codes of the shell

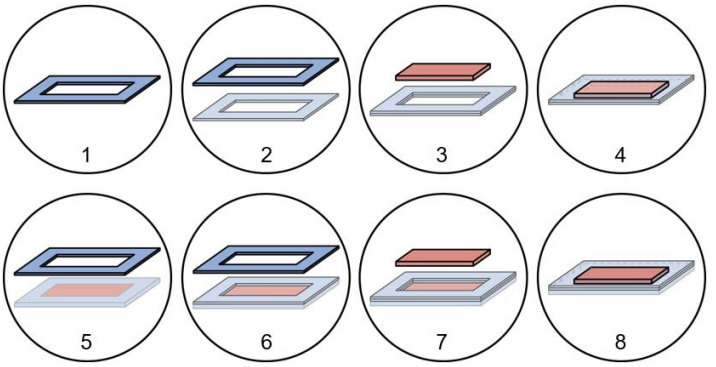


FIG. 3. — Exemplary illustration of a G-Code for the AME process.

and component, which are generated in the freeware Slic3r, are imported one after the other, presorted, and postprocessed. Postprocessing includes removal of individual G-Code commands that disturb the process and the identification of crossings without printing in the G-Code of the rubber component. Finally, the presorted and postprocessed G-Codes are merged into one common code.

Figure 3 illustrates the composition of an exemplary G-Code for the AME process with a printing strategy of the type xA→B→xA→B, in which two layers of the shell and then one layer of the component are always printed. In the following, the generation by the sorting algorithm is described step by step.

*Presorting of the Component G-Code*. — First, the entire G-Code of the component is imported line by line and searched for the end of the start sequence and the beginning of the end sequence. The general settings for 3D printing are stored in these two sections. Only lines within this area are relevant for sorting, because this area contains the traversing and extrusion commands for all layers. Finally, the lines of the start and end sequences are inserted before and after the sorted area. The G-Code follows a scheme in which each layer is initiated by a layer change command, which is then followed by all traversing and extrusion commands of this layer. The algorithm takes advantage of this fact and divides the G-Code into two lists. In the first list, all travel and extrusion commands of a layer are grouped into blocks, and in the second list, all layer change commands are stored. Once the entire G-Code has been processed, both lists contain as many entries as there are layer changes.

*Presorting of the Shell G-Code*. — The procedure for presorting the shell G-Code differs from that of the component G-Code, because the generation of the component G-Code is already performed differently in Slic3r. To avoid the generation of support structures at overhangs inside the shell, the model of the component is positioned inside the shell and both geometries are sliced with a layer thickness of the shell as a multimaterial print. The resulting G-Code shows areas of the shell as well as areas of the inner component, which are identified by the tool change commands T0 and T1. Because the G-Code of the component with a higher layer thickness has already been generated and presorted, only the part of the shell that gets initiated by the T0 command is required from this G-Code.

Presorting of the shell G-Code is a two-step process. At first, the G-Code is searched line by line for a layer change and the tool change commands T0 and T1. All areas of the shell belonging to extruder T0 are stored inside a list together with the layer change commands. In the second step, the G-code is then presorted according to an analogous procedure as for the G-code of the component.

*Detect Crossings without Printing in the Component G-Code*. — When an extruder is repositioned within a layer, it is done, without printing, by crossings. A crossing consists of a move command without an extrusion command. In contrast to the thermoplastic extruder, the rubber extruder cannot differentiate between crossings and normal extrusion commands. To ensure that no rubber is extruded during crossings, the rubber extruder must be switched off before a crossing starts and switched on again after a crossing. The detection of crossings is done by the speed information F7800 in the move command of the G-Code. If this is detected, the commands for switching the extruder on and off are inserted before and after that line.

*Merging to One G-Code*. — Once the G-Codes of the component and shell have been sorted and postprocessed, they are merged into one common G-Code in a two-stage process. In the first step, the layers are sorted that belong to the bottom of the shell and therefore only to the thermoplastic extruder. A shell bottom is present if the input thickness of the bottom of the shell is greater than 0. However, if the thickness of the bottom is 0, then there is only a vertical shell and no bottom, so that the second step of sorting can be started immediately.

The second step sorts the area in which the layers of the shell and component alternate. In this case, the shell is printed first in each layer, and if the G-codes of the component and shell have different layer thicknesses, it is necessary to print as many layers of the shell until they have the same thickness as one layer of the component. Following this procedure, the layers of the shell and the layers of the component are printed alternately until all blocks of the component have been sorted. The required tool change command is inserted before each block. Finally, the lines belonging to the start and end sequence are inserted before and after the sorted area. In the end, all lines are exported as a common G-Code.

## ANALYSIS OF THE PRINTED COMPONENTS

Tests were carried out to determine the optimal vulcanization time. At 150 °C, the vulcanization time $t_{90}$ was 7 min 20 s. This duration was used for the manufacturing of a reference sample in a conventional heat press process. However, it has to be considered that heat transfer inside the hot-air autoclave is significantly lower than inside the heating press, so that the vulcanization time has to be increased. To manufacture the reference samples, S2-tensile specimens were stamped out from a rubber plate of 2 mm thickness and manufactured in a heating press at a temperature of 80 °C and a pressure of 280 bar for several minutes. At this temperature, vulcanization is not yet initiated. The stamped-out test specimens were vulcanized in the autoclave with five different time periods at 150 °C and 7 bar. In Table I, the results of the tensile test for the vulcanized specimen are compared with the unvulcanized specimen and the vulcanized reference sample.

Comparing the value of the unvulcanized specimen with the values of the vulcanized specimens, it is obvious that the curing process in the autoclave was successful. The reference sample provides a tensile strength of 21.9 MPa and an elongation at break of 462%. Here, the sample with 7 and 15 min vulcanization time, respectively, shows the most similar material behavior with a tensile strength of 23.7 MPa and 568% elongation at break and 22.8 MPa and 513%, respectively, which are in the range of error. The latter shows a stronger increase of stress by increasing stress, which might be observed due to a more homogeneous curing process. By further increasing the time inside the autoclave, the values of the maximum tensile strength decrease significantly due to reversion of the natural rubber as well as maximum elongation at break. Because of the increasing stress values at 100% strain with longer vulcanization time, it can be assumed that an embrittlement of the material occurs. For that reason, 15 min was set as the vulcanization time in the autoclave for further tests.

TABLE I
VARIED VULCANIZATION TIME OF NR-BASED RUBBER MIXTURE AT 150 °C

| Vulcanization time, min | Tensile strength, MPa | Elongation at break, % | Stress at 100% strain, MPa | Stress at 200% strain, MPa | Stress at 300% strain, MPa |
|---|---|---|---|---|---|
| 0 | 0.8 ± 0.1 | 205 ± 60 | 0.5 ± 0.1 | 0.7 | — |
| 7 | 23.7 ± 4.4 | 568 ± 7 | 1.5 ± 0.4 | 3.9 ± 0.9 | 7.2 ± 1.5 |
| 15 | 22.8 ± 2.1 | 513 ± 40 | 2.3 ± 0.2 | 5.6 ± 0.4 | 9.7 ± 0.5 |
| 30 | 12.0 ± 1.4 | 325 ± 40 | 2.7 ± 0.1 | 6.3 ± 0.2 | 10.4 ± 0.2 |
| 45 | 7.1 ± 1.7 | 220 ± 40 | 2.6 ± 0.1 | 6.2 ± 0.2 | — |
| 60 | 6.5 ± 0.4 | 209 ± 13 | 2.7 ± 0.1 | 6.0 ± 0.2 | — |
| Reference sample | 21.9 ± 4.1 | 462 ± 60 | 2.7 ± 0.1 | 6.3 ± 0.1 | 10.8 ± 0.1 |

All 3D-printing tests with rubber were carried out with a nozzle diameter of 1 mm, resulting in a strand diameter of 1.3 mm due to swelling.[26] A smaller nozzle diameter and thus a higher print resolution was not possible with the selected rubber compound and the extruder used since the extruder reached its torque limit. A decrease in viscosity of the used rubber mixture to enable extrusion through a smaller nozzle is limited by the following aspects and can be the content of further studies. First, the reduction of carbon black content as a filler would lower the filler–filler network stability and cause a stronger distortion of the extrudate,[21] such that the dimensional stability cannot be ensured despite the presence of a thermoplastic shell. Second, low-viscous feeding stripes tear off in the feeding zone due to insufficient screw design, which influences the intake behavior and results in an instable volume flow.

For the first printing tests, the nozzle distance to the table was set to 0.9 mm, which is slightly smaller than the stripe diameter of about 1.3 mm, squeezing the rubber strand onto the printing plate. This causes the stripes to be wider. The temperature of the extruder was set to 100 °C and the rotational speed was set to 40 rpm, which correspond to a printing velocity of 1.98 mm/s. Before first printing the geometrically complex parts, the influence of the distance between the two printed stripes on the mechanical properties had to be investigated. Therefore, the additive manufactured rubber plates consisting of two additively manufactured rubber layers with different stripe distances from 1.2 to 1.6 mm were manufactured in a parallel printing pattern to observe the influence of adhesion of neighboring stripes. A filling density of 100% was adjusted in the slicing software.

The tensile test specimens were stamped out of the respective plate, vulcanized, and tested at a 90° angle to the printing direction, which is illustrated in Figure 4.

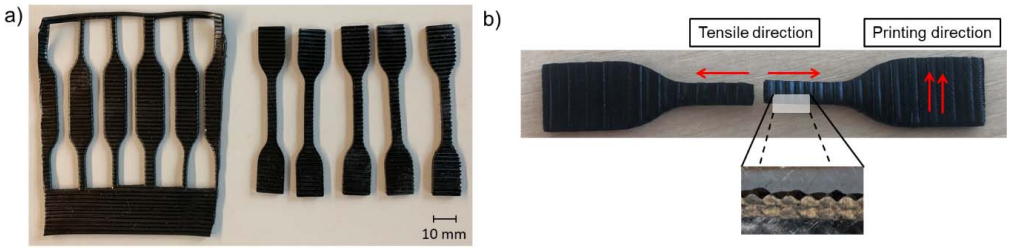


FIG. 4. — S2 tensile specimens. (a) Stamped-out specimen before vulcanization. (b) Scheme of a single S2 specimen after a tensile test (test direction perpendicular to print direction, parallel printing pattern).

TABLE II
TENSILE TESTS OF S2 SPECIMENS TO DETERMINE THE OPTIMAL STRIPE DISTANCE

| Test specimen | Tensile strength, MPa | Elongation at break, % | Stress at 100% strain, MPa | Stress at 200% strain, MPa | Stress at 300% strain, MPa | Deviation from standard thickness, % |
|---|---|---|---|---|---|---|
| Reference sample | 21.9 ± 4.1 | 462 ± 60 | 2.7 ± 0.1 | 6.3 ± 0.1 | 10.8 ± 0.1 | 0 |
| 1.2 mm nozzle distance | 16.5 ± 1.2 | 495 ± 19 | 1.6 ± 0.1 | 4.0 ± 0.2 | 7.4 ± 0.3 | Approx. +30 |
| 1.4 mm nozzle distance | 13.9 ± 1.1 | 421 ± 20 | 1.8 ± 0.1 | 4.5 ± 0.2 | 8.1 ± 0.3 | Approx. +0.5 |
| 1.6 mm nozzle distance | 12.7 ± 0.5 | 406 ± 30 | 1.7 ± 0.2 | 4.3 ± 0.3 | 7.8 ± 0.5 | Approx. −15 |

The values of the tensile tests are shown in Table II. The highest tensile strength shows the sample with a stripe distance of 1.2 mm as well as a maximum elongation at break (495%). During the printing process, the stripes in each single layer have the greatest overlap among each other, which leads to a higher stability of the additive manufactured part. However, the deviation of the standard thickness is very high (+30%). The best dimensional accuracy provides a sample of 1.4 mm stripe distance, showing reasonable values of tensile strength of 13.9 MPa and 421% elongation at break. If the stripe distance is further increased, the mechanical properties decrease.

To neglect the adhesion of the stripes among each other, samples were manufactured with a 1.4 mm stripe distance and were tested for their tensile properties in the printing direction. Also, further S2 specimens were manufactured, using a crossed-printing strategy, which means that the layers were printed in an alternating angle of 90°, improving the isotropy of the sample. In this case, two different tests were performed. In one test, the upper layer was teared in the printing direction, and in the other test, the lower layer was teared. The results of the tensile tests are shown in Table III.

TABLE III
TENSILE TESTS OF S2 SPECIMENS WITH DIFFERENT PRINTING PATTERNS

| Printing strategy of the specimen | Tensile strength, MPa | Elongation at break, % | Deviation from standard thickness, % |
|---|---|---|---|
| Reference sample | 21.9 ± 4.1 | 462 ± 60 | — |
| Parallel; test direction is printing direction | 24.8 ± 2.4 | 580 ± 50 | Approx. +10 |
| Crossed; printing direction of upper layer in test direction | 13.6 ± 0.5 | 470 ± 12 | Approx. +25 |
| Crossed; printing direction of lower layer in test direction | 14.3 ± 0.8 | 453 ± 20 | Approx. +30 |
| Parallel; test direction is 90° to printing direction | 13.9 ± 1.1 | 421 ± 20 | Approx. +0.5 |

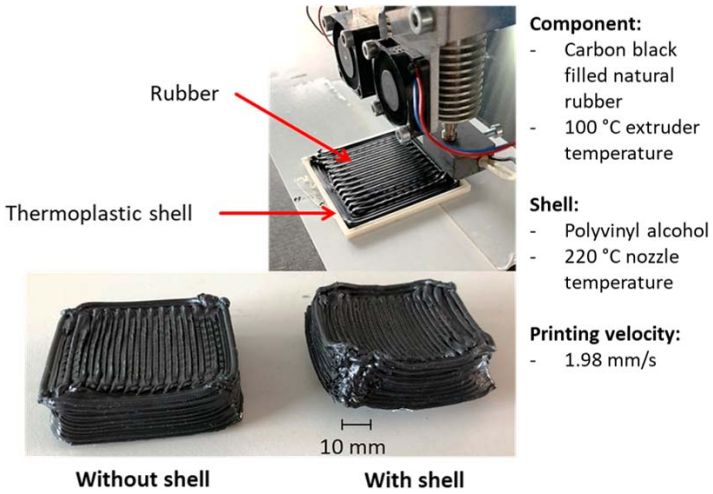


FIG. 5. — Comparison of an additively manufactured rubber part with and without thermoplastic shell.

From Table III, it can be deduced that the highest tensile strength and elongation at break (24.8 MPa, 580%) are obtained when the specimen is teared in the direction of printing. That is because the main contribution to the mechanical stability is provided by the material properties, rather than the quality of the adhesion between the stripes after additive manufacturing. Otherwise, the crossed-printing patterns reveal a better anisotropic behavior and show no significant difference between the order of the printed layers. However, the mechanical properties are lower compared with the specimen that is printed parallelly and tested in the printing direction. To investigate better the influence of the printing strategies, parts with more layers have to be manufactured to determine whether an improvement can be achieved. The tensile strength of the crossed test specimens is reduced by about 44% compared with the noncrossed sample, which is teared in the printing direction.

To print more complex and voluminous rubber parts, the first printing tests of rubber cuboids with a dimension of 50 mm × 50 mm × 9.9 mm were carried out. The initial adhesion, especially of the rubber part to the printing bed, is challenging, so that double-sided adhesive tape had to be attached to the printing bed for increased adhesion. The shell is built up using a concentric printing strategy, whereas the rubber part is printed in a crossed-printing pattern from one layer to another, except for three concentrically surrounding layers.

In Figure 5, the effect of the thermoplastic shell on the additive manufactured rubber part is illustrated. Both parts, with and without a thermoplastic shell, could be printed successfully. It is obvious that in this case for geometrically simple parts, a shell structure is not required.

Shells gain in importance for components with bridges or overhangs. In addition, an accelerated curing system could improve dimensional stability due to scorching either immediately after the printing process or in the autoclave in a second step. However, scorching inside the extruder has to be prevented. Moreover, scorching directly after passing the nozzle might lower the adhesion between the printed layers due to reduced flowability. Furthermore, the increased printing temperature of 220 °C for the HT-PVA leads to a significant heat conduction into the rubber part, resulting in an enhanced heat distortion. The use of a heating system for the chamber volume of the 3D printer could prevent a cool down of the already printed rubber layers. Thus, the temperature difference of rubber and thermoplastic is decreased, which might reduce the heat distortion and

increase the dimensional stability as well. However, this may lower the adhesion of the first printing layer on the bed by melting the glue of the double-sided adhesive tape.

Another approach would be the use of a thermoplastic material with a significantly lower melting point, allowing lower processing temperatures during additive manufacturing. However, it is important to note that the dimensional stability of this thermoplastic material may no longer be sufficient for the additively manufactured rubber part at the vulcanization temperatures used in the autoclave. Because of the early melting of the thermoplastic shell, the rubber compound, which is still flowable at the beginning of the vulcanization process, could lose the desired geometric shape.

## CONCLUSION

This article deals with the development, construction, and testing of a 3D-printing system for additive manufacturing of rubber parts. It has been demonstrated that the main principle of the AME process for additive manufacturing of carbon black–filled rubber parts is a promising technology. The developed system is based on a 3D printer for the additive manufacturing of thermoplastic components from BZT Maschinenbau GmbH. In addition, a 9 mm twin-screw extruder from Three-Tec GmbH is used to allow rubber printing. The rubber strips are fed continuously. The 3D printer enables the additive production of rubber compounds and thermoplastics in a serial process by alternately printing thin layers of thermoplastics for the shell and rubber for the component.

The process chain of the AME process was described as a six-stage process. First, a desired rubber part has to be designed and converted into STL format. Second, a thermoplastic shell is automatically generated using computer-aided technology. Afterward, the printable G-Codes of the part and its shell are generated separately. The G-Codes are merged by a program in a way that each printed layer of thermoplastic is followed by a layer of rubber. With a higher resolution of the thermoplastic, several layers of thermoplastic are printed first before a layer of rubber follows. The program generates blocks for both G-Codes with a single printing layer depending on the height coordinate $z$ before merging them to a printing strategy of the type xA→B→xA→B. The following vulcanization of the rubber component in its thermoplastic shell is then performed inside an external autoclave process. Finally, the rubber part is removed from its shell, and if necessary, postprocessing is carried out.

The NR-based rubber plates were printed with an extruder temperature of 100 °C and a distance of 0.9 mm between the nozzle and the printing bed and subsequently vulcanized in the autoclave at 150 °C and 7 bar for 15 min. By using the stamped-out tensile specimens from the rubber plates, it was determined that a strand spacing of 1.4 mm within each printed layer is recommended. Ultimately, with an ideal print sample, the additively produced samples achieve a comparable tensile strength to conventionally produced samples. It has been demonstrated that shells are not necessary for simple components because, at least for the rubber compound used, the viscosity is high enough to prevent flow behavior after additively manufacturing. Moreover, the use of shells is difficult, as there is an additional heat input into the rubber components, which can lead to heat distortion. Therefore, shells should be used only for components with bridges or overhangs or if the rubber compounds used feature a lower viscosity and an increased flow behavior immediately after additive manufacturing of the strand.

## ACKNOWLEDGEMENTS

The authors thank the German Federation of Industrial Research Associations Otto von Guericke e.V. (AiF) and its member association Deutsche Kautschuk Gesellschaft e.V. (DKG) for financial support provided for work on IGF project 20527 N, funded by the Federal Ministry for

Economic Affairs and Energy (BMWi). We also like to thank Three-Tec GmbH for technical support to implement the twin screw extruder in an additive manufacturing process.

## REFERENCES

[1]T. T. Wohlers, *Wohlers Report 2012. Additive Manufacturing and 3D Printing State of the Industry: Annual Worldwide Progress Report*, Wohlers Associates, Fort Collins, CO, 2012.

[2]K. Elkins, H. Nordby, C. Janak, R. W. Gray IV, J. Helge Bohn, and D. G. Baird, 1997 International Solid Freeform Fabrication Symposium, 1997.

[3]J. Stieghorst, D. Majaura, H. Wevering, and T. Doll, *ACS Appl. Mater. Interfaces* **8**, 8239 (2016).

[4]L.-Y. Zhou, Q. Gao, J.-Z. Fu, Q.-Y. Chen, J.-P. Zhu, Y. Sun, and Y. He, *ACS Appl. Mater. Interfaces* **11**, 23573 (2019).

[5]F. Asai, T. Seki, A. Sugawara-Narutaki, K. Sato, J. Odent, O. Coulembier, J.-M. Raquez, and Y. Takeoka, *ACS Appl. Mater. Interfaces* **12**, 46621 (2020).

[6]T. J. Hinton, A. Hudson, K. Pusch, A. Lee, and A. W. Feinberg, *ACS Biomater. Sci. Eng*. **2**, 1781 (2016).

[7]F. Alkadi, J. Lee, J.-S. Yeo, S.-H. Hwang, and J.-W. Choi, *Int. J. Precis. Eng. Manuf. Green Tech*. **6**, 211 (2019).

[8]W.-G. Drossel, J. Ihlemann, R. Landgraf, E. Oelsch, and M. Schmidt, *Polymers* **12**, 2266 (2020).

[9]W.-G. Drossel, J. Ihlemann, R. Landgraf, E. Oelsch, and M. Schmidt, *Materials* **14**, 1337 (2021).

[10]T. R. Vijayaram, *Int. J. Design Manufact. Technol*. 3, 25 (2009).

[11]A. Nakamura, A. Kasuga, and H. Arai, *Construct. Build. Mater*. **12**, 115 (1998).

[12]D. Nelson, *J. Eco. History* **47**, 329 (1987).

[13]F. Röthemeyer and F. Sommer, *Kautschuk Technologie. Werkstoffe - Verarbeitung - Produkte*, Hanser, München, Germany, 2013.

[14]J.-P. Kruth, M. C. Leu, and T. Nakagawa, *CIRP Ann*. **47**, 525 (1998).

[15]S. H. Khajavi, J. Partanen, and J. Holmström, *Comput. Indust*. **65**, 50 (2014).

[16]S. Ford and M. Despeisse, *J. Clean. Prod*. **137**, 1573 (2016).

[17]W. W. Wits, J. R. R. García, and J. M. J. Becker, *Proc. CIRP* **40**, 693 (2016).

[18]K. Reincke, B. Langer, S. Döhler, U. Heuert, and W. Greilmann, *KGK Kautschuk Gummi Kunststoffe* **2014**, 60 (2014).

[19]S. Phogat and A. K. Gupta, *J. Qual. Maint. Eng*. **25**, 25 (2019).

[20]C. H. Schroeder, RUBBER CHEM. TECHNOL. **25**, 651 (1952).

[21]J. L. White and J. W. Crowder, *J. Appl. Polym. Sci*. **18**, 1013 (1974).

[22]H. Wittek, B. Klie, U. Giese, S. Kleinert, L. Bindszus, and L. Overmeyer, *KGK-Kautschuk Gummi Kunststoffe* **72**, 53 (2019).

[23]S. S. Crump, U.S. Patent 5,121,329A, June 9, 1992.

[24]S. S. Crump, J. W. Comb, W. R. Priedeman Jr, and R. L. Zinniel, U.S. Patient 5,503,785A April 2, 1996.

[25]L. Sundermann, S. Leineweber, B. Klie, U. Giese, and L. Overmeyer, *KGK-Kautschuk Gummi Kunststoffe* **73**, 30 (2020).

[26]C. Price, *Proc. R. Soc. Lond. A* **351**, 331 (1976).

[*Received October 2020, Revised June 2021*]